

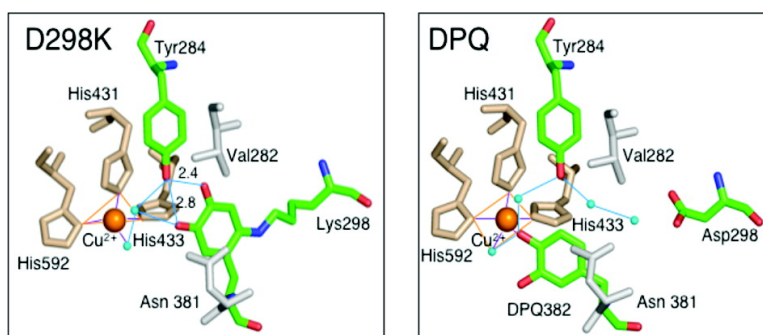
Article

Trapping of a Dopaquinone Intermediate in the TPQ Cofactor Biogenesis in a Copper-Containing Amine Oxidase from *Arthrobacter globiformis*

Robyn H. Moore, M. Ashley Spies, Matthew B. Culpepper, Takeshi Murakawa, Shun Hirota, Toshihide Okajima, Katsuyuki Tanizawa, and Minae Mure

J. Am. Chem. Soc., **2007**, 129 (37), 11524-11534 • DOI: 10.1021/ja0731165 • Publication Date (Web): 23 August 2007

Downloaded from <http://pubs.acs.org> on February 14, 2009



More About This Article

Additional resources and features associated with this article are available within the HTML version:

- Supporting Information
- Access to high resolution figures
- Links to articles and content related to this article
- Copyright permission to reproduce figures and/or text from this article

[View the Full Text HTML](#)

Trapping of a Dopaquinone Intermediate in the TPQ Cofactor Biogenesis in a Copper-Containing Amine Oxidase from *Arthrobacter globiformis*

Robyn H. Moore,[§] M. Ashley Spies,^{†,‡} Matthew B. Culpepper,[§] Takeshi Murakawa,^{†,#} Shun Hirota,^{||} Toshihide Okajima,[†] Katsuyuki Tanizawa,^{*,†} and Minae Mure^{*,§}

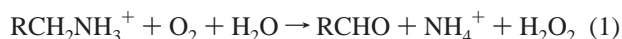
Contribution from the Department of Chemistry, University of Kansas, Lawrence, Kansas 66045, Department of Structural Molecular Biology, Institute of Scientific and Industrial Research, Osaka University, Ibaraki, Osaka 567-0047, Japan, and Graduate School of Materials Science, Nara Institute of Science and Technology, Nara 630-0192, Japan and PRESTO, JST, Saitama 332-0012, Japan

Received May 3, 2007; E-mail: mmure@ku.edu; tanizawa@sanken.osaka-u.ac.jp

Abstract: The biogenesis of the topaquinone (TPQ) cofactor of copper amine oxidase (CAO) is self-catalyzed and requires copper and molecular oxygen. A dopaquinone intermediate has been proposed to undergo 1,4-addition of a copper-associated water molecule to form the reduced form of TPQ (TPQ_{red}), followed by facile oxidation by O₂ to yield the mature TPQ (TPQ_{ox}). In this study, we have incorporated a lysine residue in the active site of *Arthrobacter globiformis* CAO (AGAO) by site-directed mutagenesis to produce D298K-AGAO. The X-ray crystal structure of D298K-AGAO at 1.7-Å resolution revealed that a covalent linkage formed between the ε-amino side chain of Lys298 and the C2 position of a dopaquinone derived from Tyr382, a precursor to TPQ_{ox}. We assigned the species as an iminoquinone tautomer (LTI) of lysine tyrosylquinone (LTQ), the organic cofactor of lysyl oxidase (LOX). The time course of the formation of LTI at pH 6.8 was followed by UV/vis and resonance Raman spectroscopies. In the early phase of the reaction, an LTQ-like intermediate was observed. This intermediate then slowly converted to LTI in an isosbestic manner. Not only is the presence of a dopaquinone intermediate in the TPQ biogenesis confirmed, but it also provides strong support for the proposed intermediacy of a dopaquinone in the biogenesis of LTQ in LOX. Further, this study indicates that the dopaquinone intermediate in AGAO is mobile and can swing from the copper site into the active-site wedge to react with Lys298.

Introduction

Copper amine oxidase (CAO) (EC1.4.3.6) catalyzes the oxidative deamination of various primary amines to produce the corresponding aldehyde concomitant with hydrogen peroxide and ammonia (eq 1).¹



CAO contains a tyrosine-derived quinone cofactor, 2,4,5-trihydroxyphenylalanine quinone (topaquinone, TPQ, see Scheme 1) in addition to the active-site copper.² The biogenesis of the TPQ cofactor is self-catalyzed and requires copper and molecular oxygen.^{3,4} The mechanism of TPQ biogenesis has been

studied for AGAO^{5–11} and a yeast CAO from *Hansenula polymorpha* (HPAO).^{12–19} The biogenesis of TPQ can be initiated by addition of Cu²⁺ to the apoprotein under aerobic conditions or exposure to O₂ of the Cu²⁺-bound precursor protein prepared under anaerobic conditions.²⁰ The copper-free tyrosine precursor (apo) form of recombinant CAO can be prepared by removing copper from the buffers used during

[§] University of Kansas.

[†] Institute of Scientific and Industrial Research, Osaka University.

^{||} Nara Institute of Science and Technology and PRESTO, JST.

[#] Current address: Department of Biochemistry, University of Illinois, Urbana, IL 61801.

^{*} Current address: Department of Biochemistry, Osaka Medical College, Takatsuki, Osaka 569-8686, Japan.

(1) Mure, M.; Mills, S. A.; Klinman, J. P. *Biochemistry* **2002**, *41* (30), 9269–9278.

(2) Janes, S. M.; Mu, D.; Wemmer, D.; Smith, A. J.; Kaur, S.; Maltby, D.; Burlingame, A. L.; Klinman, J. P. *Science* **1990**, *248* (4958), 981–987.

(3) Matsuzaki, R.; Fukui, T.; Sato, H.; Ozaki, Y.; Tanizawa, K. *FEBS Lett.* **1994**, *351* (3), 360–364.

(4) Cai, D.; Klinman, J. P. *J. Biol. Chem.* **1994**, *269* (51), 32039–32042.

(5) Ruggiero, C. E.; Smith, J. A.; Tanizawa, K.; Dooley, D. M. *Biochemistry* **1997**, *36* (8), 1953–1959.

(6) Ruggiero, C. E.; Dooley, D. M. *Biochemistry* **1999**, *38*, 2892–2898.

(7) Nakamura, N.; Matsuzaki, R.; Choi, Y. H.; Tanizawa, K.; Sanders-Loehr, J. *J. Biol. Chem.* **1996**, *271* (9), 4718–4724.

(8) Wilce, M. C.; Dooley, D. M.; Freeman, H. C.; Guss, J. M.; Matsunami, H.; McIntire, W. S.; Ruggiero, C. E.; Tanizawa, K.; Yamaguchi, H. *Biochemistry* **1997**, *36* (51), 16116–16133.

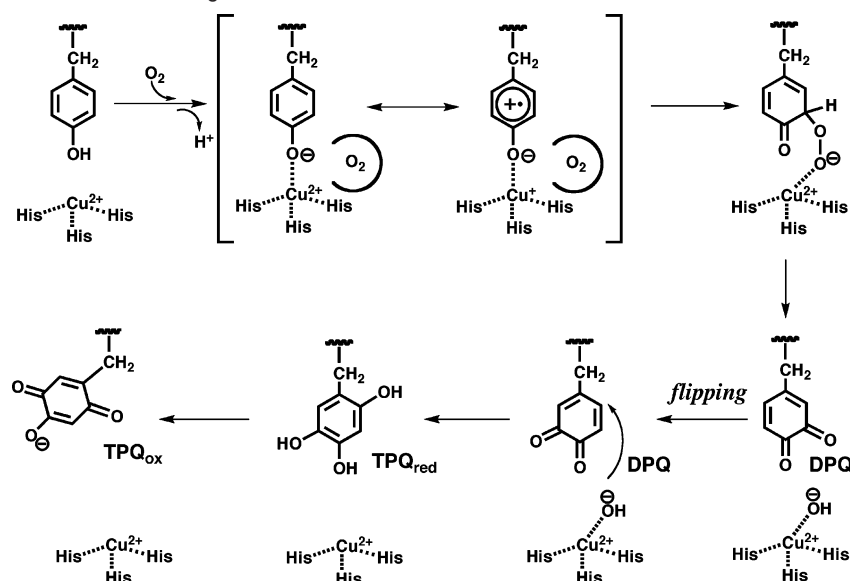
(9) Kim, M.; Okajima, T.; Kishishita, S.; Yoshimura, M.; Kawamori, A.; Tanizawa, K.; Yamaguchi, H. *Nat. Struct. Biol.* **2002**, *9* (8), 591–596.

(10) Matsunami, H.; Okajima, T.; Hirota, S.; Yamaguchi, H.; Hori, H.; Mure, M.; Kuroda, S.; Tanizawa, K. *Biochemistry* **2004**, *43*, 2178–2187.

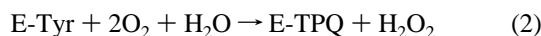
(11) Okajima, T.; Kishishita, S.; Chiu, Y.-C.; Murakawa, T.; Kim, M.; Yamaguchi, H.; Hirota, S.; Kuroda, S.; Tanizawa, K. *Biochemistry* **2005**, *44*, 12041–12048.

(12) Hevel, J. M.; Mills, S. A.; Klinman, J. P. *Biochemistry* **1999**, *38*, (12), 3683–3693.

(13) Schwartz, B.; Dove, J. E.; Klinman, J. P. *Biochemistry* **2000**, *39* (13), 3699–3707.

Scheme 1. Proposed Mechanism for TPQ Biogenesis¹⁷

purification. In AGAO, the stoichiometry of O₂ consumption to hydrogen peroxide formation was determined where 2 mol equiv of O₂ were consumed and 1 mol of H₂O₂ was produced per 1 mol of TPQ formed (eq 2).⁶ Mechanisms have been proposed that account for this stoichiometry (e.g., Figure 1).



In 2004, an X-ray snapshot analysis was performed in an attempt to freeze trap the reaction intermediates of TPQ biogenesis in AGAO (Figure 1).⁹ The structure of the apo form of AGAO revealed that the phenolic hydroxyl group of the precursor tyrosine (Tyr382) pointed toward the vacant metal site composed of the three conserved histidine residues (His431, His433, and His592).^{8,9} When apoprotein crystals were soaked with copper anaerobically, copper was bound in a tetrahedral geometry to the three His ligands and Tyr382 provided the fourth ligand (Figure 1a). Upon exposure of the copper-bound crystals to molecular oxygen two copper-bound intermediates (proposed to be dopaquinone (DPQ, Figure 1b) and trihydroxybenzene (TPQ_{red}, Figure 1d), respectively) were detected where the O4 hydroxyl group of the aromatic ring remained directly coordinated to Cu²⁺. During the conversion of the putative dopaquinone to TPQ_{red}, the aromatic ring rotated 180° to undergo hydration by copper-associated water (Figure 1c). In the final step of the oxidation of TPQ_{red} to TPQ_{ox}, the TPQ ring finally moved off Cu²⁺ to leave the cofactor in the active conformation (Figure 1e). As a result of the conformational changes during biogenesis, the TPQ ring in the mature AGAO is in a different orientation from the precursor tyrosine (Figure 1a). In the mature AGAO, the O5 carbonyl group of TPQ_{ox} is facing the proposed substrate entry channel⁸ and the conserved

aspartate residue (Asp298) (assigned as an active-site base¹¹), and the O2 carbonyl group interacts with the copper through a conserved water molecule, but neither O2 nor O5 are directly ligated to the copper. This orientation of the TPQ ring is critical for the optimal activity of CAO.²¹ In the active (holo) form of AGAO, two water molecules are associated with the copper [one is on the Jahn–Teller axis (W_a) and the other is in the equatorial position (W_e)], in addition to the three histidines to provide a distorted square pyramidal coordination geometry.²²

Detailed kinetic and spectroscopic studies on the biogenesis of TPQ in HPAO revealed that the rate-determining step is the formation of a species absorbing at 350 nm that is proposed to be a Cu²⁺–tyrosinate complex that exists in equilibrium with a Cu¹⁺–tyrosyl radical (Scheme 1).¹⁶ The absence of a kinetic isotope effect on the rate of TPQ formation using the 3,5-ring dideuterated tyrosine precursor precluded that the subsequent C–H bond cleavage step from a proposed Cu²⁺–arylperoxide intermediate was rate limiting (Scheme 1).¹⁷ No spectroscopic intermediates were detected during the conversion of the 350-nm species to mature TPQ_{ox} absorbing at 472 nm. In AGAO, binding of Cu²⁺ to the precursor protein under anaerobic conditions does not lead to the formation of any distinct new features in the UV/vis spectrum, in contrast to HPAO.⁵ When O₂ was introduced to the system, rapid formation of mature TPQ_{ox} (478 nm) was observed, where the reaction was complete within a couple of minutes.

Lysyl oxidase (LOX) is also a copper-containing amine oxidase but differs from CAO by being monomeric (32 kDa) and having a lysine tyrosylquinone (LTQ, see Scheme 2) cofactor.²³ A model study suggested that 1,4-addition of the ε-amino side chain of lysine to the dopaquinone intermediate can form the LTQ cofactor, where the active site of LOX must be pre-organized to achieve the selectivity of the reaction (Scheme 2).²⁴ Recently, Bollinger et al. isolated the copper-

(14) Dove, J. E.; Schwartz, B.; Williams, N. K.; Klinman, J. P. *Biochemistry* **2000**, *39* (13), 3690–3698.

(15) Schwartz, B.; Olgin, A. K.; Klinman, J. P. *Biochemistry* **2001**, *40*, 2954–2963.

(16) DuBois, J. L.; Klinman, J. P. *Arch. Biochem. Biophys.* **2005**, *433*, 255–265.

(17) DuBois, J. L.; Klinman, J. P. *Biochemistry* **2005**, *44*, 11381–11388.

(18) Samuels, N. M.; Klinman, J. P. *Biochemistry* **2005**, *44*, 14308–14317.

(19) DuBois, J. L.; Klinman, J. P. *Biochemistry* **2006**, *45*, 3178–3188.

(20) DuBois, J. L.; Klinman, J. P. *Methods Enzymol.* **2004**, *378*, 17–31.

(21) Mure, M. *Acc. Chem. Res.* **2004**, *37* (2), 131–139.

(22) Kishishita, S.; Okajima, T.; Kim, M.; Yamaguchi, H.; Hirota, S.; Suzuki, S.; Kuroda, S.; Tanizawa, K.; Mure, M. *J. Am. Chem. Soc.* **2003**, *125*, 1041–1055.

(23) Wang, S. X.; Mure, M.; Medzihradzky, K. F.; Burlingame, A. L.; Brown, D. E.; Dooley, D. M.; Smith, A. J.; Kagan, H. M.; Klinman, J. P. *Science* **1996**, *273* (5278), 1078–1084.

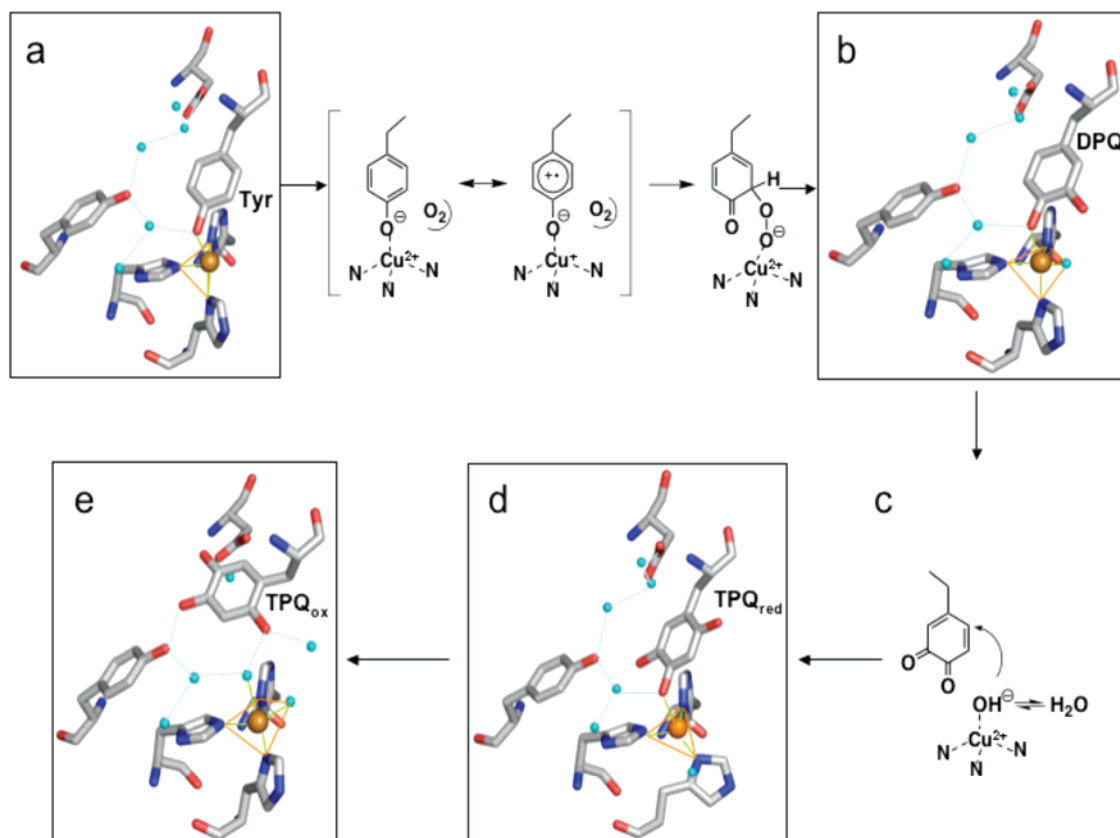
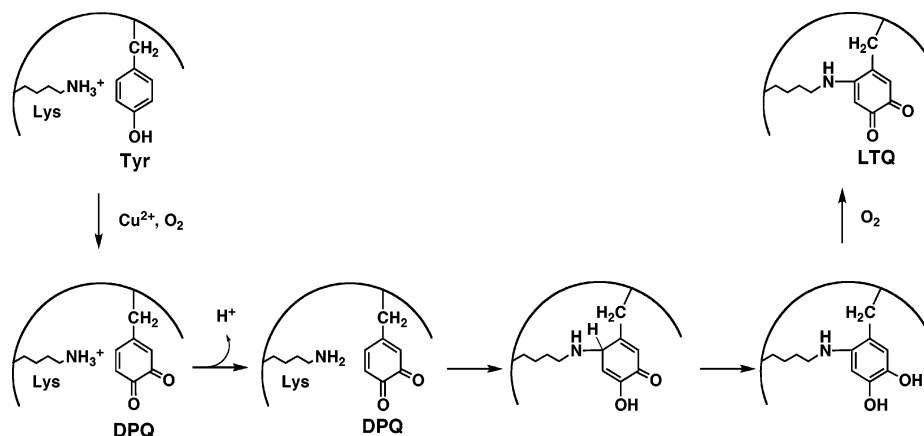


Figure 1. Proposed mechanism of TPQ biogenesis. Panels a, b, d, e are intermediates observed in the X-ray snapshot analysis.⁹ Copper is shown as a golden sphere, and water molecules are shown in light-blue spheres. (a) Tyr: Tyr382 precursor, (b) DPQ: dopaquinone, (c) proposed DPQ in a flipped form, (d) TPQ_{red}: 2,4,5-trihydroxylbenzene form of the reduced TPQ, (e) TPQ_{ox}: the oxidized form of TPQ. Figures are generated by Pymol (DeLano Scientific LLC, <http://www.pymol.org>).

Scheme 2. Proposed Mechanism for LTQ Biogenesis^{23–25}



free precursor form of recombinant LOX (apo-LOX) and showed the formation of the LTQ cofactor by extensive dialysis of the apo-LOX against copper under aerobic conditions.²⁵ They proposed that the biogenesis of the LTQ cofactor is a self-catalyzed process requiring only Cu²⁺ and molecular oxygen as in the case of the TPQ cofactor in CAOs. Taken together, these results support proposals that both TPQ and LTQ biogenesis proceed through a dopaquinone intermediate. However, to date there has been no definitive identification of dopaquinone in either CAO or LOX.

In this study, we have incorporated a lysine residue into the active site of AGAO by site-directed mutagenesis in an attempt to chemically trap the putative dopaquinone intermediate in both the unflipped (Figure 1b) and flipped (Figure 1c) conformations. Asp298 and Met602 were chosen as the sites of mutation since they are close to the C2 position of each dopaquinone intermediate. D298K and M602K-AGAOs were prepared and purified to homogeneity. Characterization of the organic cofactor in D298K by UV/vis and resonance Raman spectroscopies, and X-ray crystallography revealed that it contains an LTQ-like

(24) Mure, M.; Wang, S. X.; Klinman, J. P. *J. Am. Chem. Soc.* **2003**, *125* (20), 6113–6125.

(25) Bollinger, J. A.; Brown, D. E.; Dooley, D. M. *Biochemistry* **2005**, *44* (35), 11708–11714.

lysine cross-linked quinone in place of the native TPQ cofactor. On the other hand, TPQ was formed in M602K. The formation of an LTQ-like quinone in D298K not only provides the first chemical evidence for the proposed intermediacy of dopaquinone during the biogenesis of TPQ but also gives strong support for the common intermediacy of dopaquinone in TPQ and LTQ biogenesis.

Materials and Methods

2-Phenylethylamine, 2-hydrazinopyridine hydrochloride, 4-nitrophenylhydrazine, and CuSO₄ were purchased from Sigma-Aldrich. Nitro blue tetrazolium used for quinone staining was purchased from CalBiochem. Synthetic oligonucleotides were purchased from Operon Biotechnologies, Inc. PCR was performed on a DNA Engine PTC-200 Peltier Thermal Cycler (Biorad). Plasmids were prepared using a QIAprep Spin Miniprep kit (Qiagen). DNA sequencing was performed at the UC Berkeley DNA sequencing facility.

Site-Directed Mutagenesis. The expression plasmids for D298K and M602K-AGAO were generated by site-directed mutagenesis using a Quikchange mutagenesis kit from Stratagene on pPEAO-02³ as a parent vector. The DNA primers used for D298K were 5'-CCTGGCA-GAACTACTTCAAGACGGGGAGTACCTGGTG-3' (forward) and 5'-CACCAGGTACTCCCCGCTTTGAAGTAGTTCTGCCAGG-3' (reverse) (underlined nucleotides correspond to the sites of mutation). The DNA primers used for M602K were 5'-GGACTGGCCCATCAAAC-CGGTGGACACCGTC-3' (forward) and 5'-GACGGTGTCCACCG-GTTTGATGGGCCAGTCC-3' (reverse). An expression plasmid for the double mutant, Y284F/D298K was generated on the D298K-AGAO expression vector using the DNA primers, 5'-GATGGTGGTCC-GTTCGGCGATCCGTC-3' (forward) and 5'-GGACGGATCGCCG-AACGGCACCACCATC-3' (reverse). All plasmids were fully sequenced, and the point mutations were confirmed.

Enzyme Purification. Wild-type (WT) and mutant AGAO expression plasmids were transformed into *Escherichia coli* CD03, a mutant strain of *E. coli* BL21(DE3) where two out of three catalase genes were disrupted.²² The mature forms of WT, D298K, M602K, and Y284F/D298K were produced by growing the transformants in LB-ampicillin media containing 50 μM Cu²⁺ and purified to homogeneity following the published procedure.²⁶ The Y284F/D298K mutant was not very stable, and the purification was performed in the minimal time (2–3 days). The precursor forms of WT, D298K, and Y284F/D298K were produced in LB-ampicillin media and purified to homogeneity using the copper-depleted buffers as described previously.^{3,22} Protein concentration was determined spectrophotometrically by using extinction coefficients at 280 nm of 12.3 and 13.2 for 1% (w/v) solutions of the apo and holo forms of AGAO, respectively.³

Activity Assay. The enzyme activity was assayed by O₂ consumption using a Clark-type polarographic electrode (Hansatech Instruments) using 2-phenylethylamine as a substrate according to the published procedure.^{3,22}

UV/Vis Spectroscopy. UV/vis spectroscopy was performed on an HP8520 photodiode array UV/vis spectrophotometer equipped with a temperature-controlled cell holder at 30 ± 0.2 °C (path length of 1 cm). The effect of 8 M urea and pH on the UV/vis absorption spectrum of D298K was studied by dialyzing the sample against the appropriate buffer at 4 °C. The biogenesis study of D298K was performed as previously described for WT.^{3,11} The rates of formation of the 500 nm and 454 nm chromophores were determined spectrophotometrically in a reaction mixture containing 0.1 mM apo-D298K and 0.5 mM CuSO₄ in 50 mM HEPES buffer at pH 6.8 both under air-saturated and O₂-saturated conditions. The observed rate constants (*k*_{obs}) for formation and decay of the 500 nm chromophore and formation of the 454 nm chromophore were calculated by fitting absorbance changes at 320,

Table 1. Statistics of Data Collection and Refinement for D298K-AGAO

	Data Collection
cell	
space group	<i>I</i> 2
unit cell dimension	
<i>a</i> , <i>b</i> , <i>c</i> (Å), β (deg)	158.01, 63.03, 184.12, 111.96
<i>d</i> _{max} – <i>d</i> _{min} (Å)	39.9–1.68 (1.74–1.68) ^a
no. of observations	689,271
no. of unique reflections	190,511 (18,830)
<i>I</i> / <i>σ</i> (<i>I</i>)	53.2 (6.6)
overall completeness (%)	99.4 (99.1)
overall <i>R</i> _{merge} (%) ^b	4.2 (33.8)
	Refinement Statistics
<i>d</i> _{max} – <i>d</i> _{min} (Å)	39.9–1.68 (1.69–1.68)
residues in the core φ, φ regions (%)	88.7
no. of non-hydrogen atoms	10873
no. of solvent atoms	1135
average temperature factor	
main-chain (Å ²)	24.7
side-chain atoms (Å ²)	27.0
solvent atoms (Å ²)	38.6
rms deviation from ideal values	
bond lengths (Å)	0.005
bond angles (deg)	1.4
residual <i>R</i> (%) ^c	18.5 (33.0)
free residual <i>R</i> (%) ^d	20.5 (35.6)

^a The numbers in parentheses present the value for the highest resolution shell. ^b $R_{\text{merge}} = \sum_i \sum_h |I_{h,i} - \langle I_h \rangle| / \sum_h \sum_i I_{h,i}$, where $I_{h,i}$ is the intensity value of the *i*th measurement of *h*, and $\langle I_h \rangle$ is the corresponding mean value of I_h for all *i* measurements. ^c $R = \sum ||F_o| - |F_c|| / \sum |F_o|$. ^d Free residual *R* is an *R* factor of the CNS refinement evaluated for 5% of the reflections that were excluded from the refinement.

454, and 550 nm plotted versus time by least-square fitting to the sum of two exponentials using Kaleidagraph (Synergy software). Average values of two independent measurements are taken.

Reaction of D298K and D298K/Y284F with 2-Hydrazinopyridine and 4-Nitrophenylhydrazine. Five molar equivalents of the hydrazine were added to the enzyme solution (pH 6.8, 50 mM HEPES buffer), and the mixture was incubated at 30 °C. The time course of the reaction was monitored on the HP8520 photodiode array spectrophotometer.

Resonance Raman Spectroscopy. Resonance Raman spectra were obtained by using an excitation of 514.5 nm with an Ar⁺ ion laser (Spectra Physics, 2017), detected with a triple polychromator (JASCO, NR-1800) and a CCD detector (Princeton Instruments). The excitation laser beam power was 70 mW. Measurements were conducted at room temperature with a spinning cell (3000 rpm). Acetone was used to calibrate the resonance Raman shift. The accuracy of the peak positions was ±1 cm⁻¹.

Crystallization, Data Collection, and Processing. The purified D298K apoprotein was incubated with 0.5 mM Cu²⁺ for 5 days to complete the cofactor biogenesis and was crystallized under the same conditions as for the wild-type AGAO.⁸ After soaking with the crystallization buffer containing 45% (v/v) glycerol (cryoprotectant), the crystal was mounted on a thin nylon loop (φ, 0.2–0.3 mm) and frozen by flash cooling at 100 K in a cold N₂ gas stream. Diffraction data sets were collected at 100 K with a synchrotron X-ray radiation (λ = 0.9 Å) using imaging plate DIP6040 (Bruker AXS) in the beam-line station BL44XU at SPring8, Himeji, Hyogo, Japan. The collected data were found to belong to space group *I*2 with unit cell dimensions comparable to those of the wild-type AGAO. The resolution range was 1.68–40 Å. The details and statistics of data collection are summarized in Table 1. The program used for the calculation of electron density maps and refinements was CNS ver 1.1. Initially, the refinements were done by temporarily introducing the TPQ structure to the model at residue 382, and water molecules were also introduced at this stage. Later the precise cofactor structure was included at residues 298 and 382 in a model based on 2*F*_o – *F*_c and *F*_o – *F*_c maps, and *F*_o – *F*_c

(26) Shimizu, E.; Ohta, K.; Takayama, S.; Kitagaki, Y.; Tanizawa, K.; Yorifuji, T. *Biosci. Biotechnol. Biochem.* **1997**, *61* (3), 501–505.

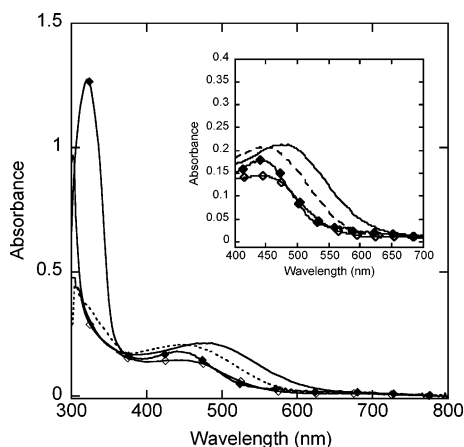


Figure 2. UV/vis absorption spectra of D298K, M602K, D298A, WT-AGAO (0.1 mM) in 50 mM HEPES buffer at pH 6.8. —◆— D298K, —◇— M602K, - - - - - D298A, — WT.

simulated annealing (sa) maps omitted for residues 298 and 382. The details and statistics of the crystallographic refinement are also given in Table 1. The atomic coordinates and structure factors for the D298K mutant of AGAO have been deposited in the Protein Data Bank with the accession code 2YX9.

Results

Designing Active-Site Mutants to Trap Dopaoquinone in TPQ Biogenesis. In an attempt to trap dopaoquinone in both the unflipped (Figure 1b) and the flipped orientations (Figure 1c), a lysine residue was incorporated at two positions in the active site of AGAO. On the basis of the X-ray crystal structure of the putative dopaoquinone intermediate,⁹ we chose to mutate Asp298 to trap the unflipped conformation (Supporting Information (SI) Figure 1). The carboxyl side chain of Asp298 is 2.3 Å from the C2 group of dopaoquinone. To determine which residue to target for the flipped conformation, we used the X-ray structure of TPQ_{red} (Figure 1d) as a model for flipped dopaoquinone. On this basis we found that Met602 is the closest residue to the C2 carbon, where the methyl group of the thioether would be 6.5 Å from the C2 of dopaoquinone (SI Figure 1).

UV/Vis Spectroscopic Properties of Holo-D298K and Holo-M602K. Figure 2 shows the UV/vis absorption spectra of D298K, M602K, and WT. The purified holo-D298K and holo-M602K were yellowish brown, which contrasts with the characteristic pink color of WT-AGAO. WT shows a typical broad absorbance with a λ_{max} at 476 nm.²² At physiological pH, the TPQ cofactor exists as a resonance-stabilized monoanion where the 4-hydroxyl group is deprotonated.²¹ The λ_{max} of the WT-AGAO reflects the extent of resonance delocalization of the O4 oxo-anion of the TPQ cofactor. The O4 of TPQ is in hydrogen-bonding contact with the conserved Tyr284, and O2 of TPQ is in hydrogen-bonding contact with two water molecules. D298K and M602K have a λ_{max} at ~450 nm that is ~30 nm blue-shifted from that of WT-AGAO. A similar 30-nm blue-shift in λ_{max} has been seen for the TPQ cofactor in D298A-AGAO²⁷ and also in D383A-ECAO²⁸ where, in these

mutants, it is likely a result of the partial localization of electrons at O4 of TPQ. In the D298A-AGAO crystal structure,²⁷ the distance between O4 and the hydroxyl group of Tyr284 is a little shorter (2.3 Å) than that seen in the WT structure (2.5 Å), consistent with a localization of the charge at O4.²² In addition to the absorbance at 450 nm, D298K also contains a prominent strong absorbance at 320 nm that is absent in WT, D298A, and M602K. Such a band has been seen for LOX isolated from bovine aorta²⁹ as well as for a recombinant form of a LOX-like protein from *Drosophila melanogaster*.²⁵ These observations suggested that the blue-shift in the visible spectrum of D298K may not simply be due to a change in charge distribution in the TPQ cofactor.

Reactivity of D298K and M602K toward Amine Substrate and Hydrazine Inhibitors.

The UV/vis spectra of D298K and M602K indicated the presence of a quinone that is different from TPQ in WT. The presence of a quinone in these mutants was determined by the standard quinone-staining method (SI Figure 2).³⁰ Both D298K and M602K were positive for quinone staining although staining was weaker than that in WT. The TPQ cofactor in CAO forms an intense chromophore with hydrazines, and the chromophore formation has been used to titrate the amount of TPQ in CAOs.³¹ In WT-AGAO, TPQ can be converted to hydrazone-azo derivatives with phenylhydrazine,²² 2-hydrazinopyridine,³² or 4-nitrophenylhydrazine.³ M602K reacted with phenylhydrazine, and the titration indicated that the protein sample contained 40% active quinone (a typical result for WT is 65% titratable). Consistent with the presence of a reactive quinone, M602K showed 20% activity toward 2-phenylethylamine in comparison to WT using a Clark O₂ electrode to assay O₂ consumption. The resonance Raman spectrum of the phenylhydrazine-derivatized M602K was very similar to that of the TPQ-phenylhydrazone adduct (SI Figure 3). This clearly indicated that the quinone in M602K is TPQ and that no cross-link had occurred between the ϵ -amino side chain of Lys602 and dopaoquinone. For this reason, we did not pursue further characterization of M602K.

In contrast to M602K and WT, the quinone in D298K did not react with any of the hydrazines where no spectral change was observed even after prolonged incubation. D298K also showed no activity toward oxidative deamination of 2-phenylethylamine. This showed that the quinone formed in D298K was trapped in a conformation that could not react with amines. This, along with the unusual UV/vis spectrum, suggested that D298K contains a quinone other than TPQ.

X-ray Crystal Structure of D298K. The structure of holo-D298K was determined by X-ray crystallography at 1.7 Å resolution (Table 1). As a result of the initial refinement, *R* and *R*_{free} values decreased to 0.200 and 0.216, respectively. The structure model except for the cofactor moiety fitted well to the $2F_o - F_c$ map (data not shown). The cross-link between the ϵ -amino group of Lys298 and the C2 atom of the side-chain aromatic ring of TPQ382 was apparent even before introducing

(27) Chiu, Y.-C.; Okajima, T.; Murakawa, T.; Uchida, M.; Taki, M.; Hirota, S.; Kim, M.; Yamaguchi, H.; Kawano, Y.; Kamiya, N.; Kuroda, S.; Hayashi, H.; Yamamoto, Y.; Tanizawa, K. *Biochemistry* **2006**, *45*, 4105–4120.
(28) Murray, J. M.; Saysell, C. G.; Wilmot, C. M.; Tambyrajah, W. S.; Jaeger, J.; Knowles, P. F.; Phillips, S. E.; McPherson, M. J. *Biochemistry* **1999**, *38* (26), 8217–8227.

(29) Tang, C.; Klinman, J. P. *J. Biol. Chem.* **2001**, *276* (33), 30575–30578.
(30) Paz, M. A.; Fluckiger, R.; Boak, A.; Kagan, H. M.; Gallop, P. M. *J. Biol. Chem.* **1991**, *266* (2), 689–692.
(31) Janes, S. M.; Palcic, M. M.; Scaman, C. H.; Smith, A. J.; Brown, D. E.; Dooley, D. M.; Mure, M.; Klinman, J. P. *Biochemistry* **1992**, *31*, 12147–12154.
(32) Mure, M.; Brown, D. E.; Saysell, C. G.; Rogers, M. S.; Wilmot, C. M.; Kurtis, C. R.; McPherson, M. J.; Phillips, S. E. V.; Knowles, P. F.; Dooley, D. M., *Biochemistry* **2005**, *44*, 1568–1582.

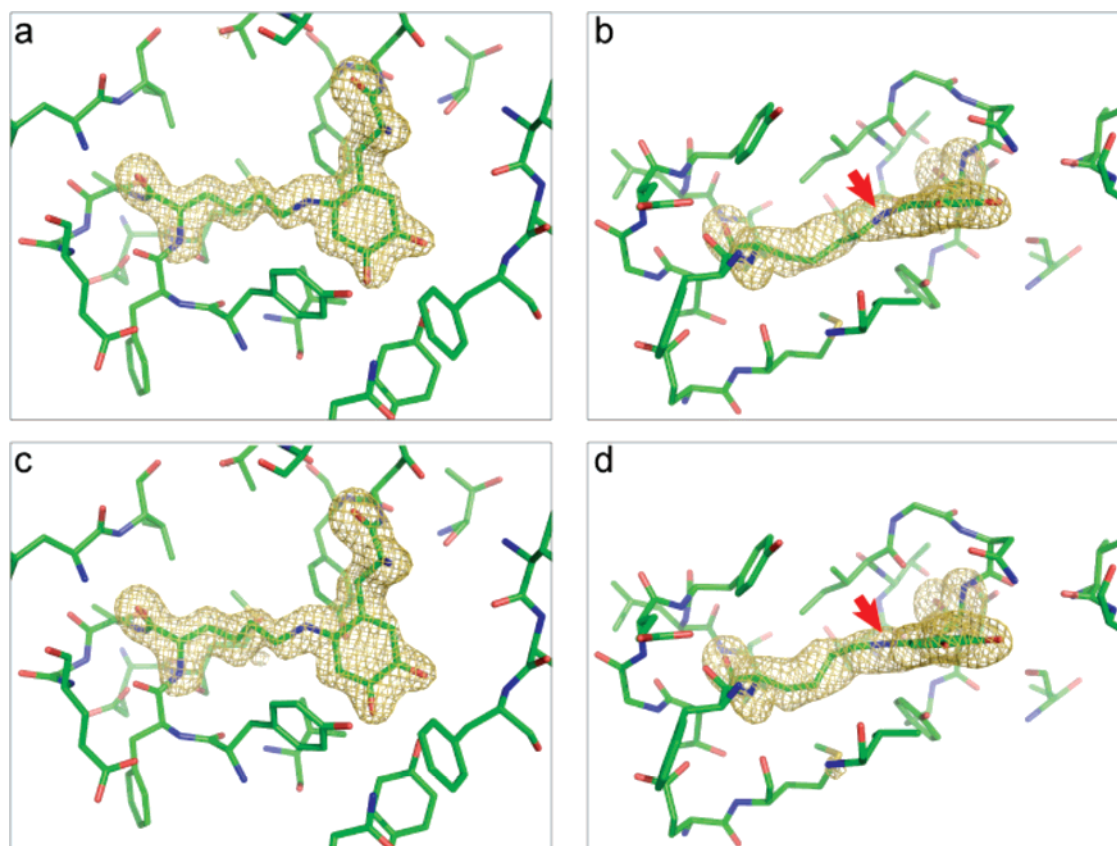
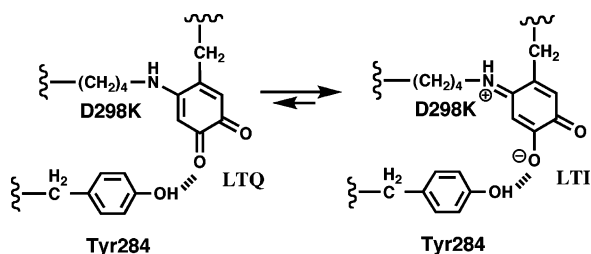


Figure 3. Electron density map of the active site of D298K. Simulated annealing (sa) omit maps (contoured at 4.5σ) are shown with the structure models of LTQ (a, b) and LTI (c, d). (a, c) Views perpendicular to the dopaquinone ring. (b, d) Views parallel to the dopaquinone ring. Red arrows show N^ϵ atoms of Lys298.

Scheme 3. Tautomerism of LTQ and LTI in D298K



the cofactor model to the residues at 298 and 382 positions. Two models including the cross-link were then examined for fitting to the electron density at residues 298 and 382. One is LTQ, and the other is the iminoquinone tautomer of LTQ (LTI) (Scheme 3). The latter model indicates that an imine bond is formed between the C2 carbon of the dopaquinone and the side-chain ϵ -amino group of Lys298. The dictionaries for these two models were created by linking the C2 atom of the dopaquinone and the ϵ -amino group of Lys298 through distinct types (single or double) of a covalent bond, whose lengths are indistinguishable crystallographically at the present resolution. After several cycles of separate refinements using the two tautomers, R and R_{free} values decreased to 0.197 and 0.214, respectively, for both models (Table 1). The extra electron density at the C5 position was very clear, suggesting a carbonyl group. The two models fitted equally well to the electron density in the $F_o - F_c$ simulated annealing (sa) omit map viewed perpendicularly to the dopaquinone ring (Figure 3a,c). However, close inspection of the lysyl side-chain portion of the models revealed that the LTI model fitted better to the omit map than the LTQ model.

Particularly in a view parallel to the dopaquinone ring, both of the N^ϵ and CE atoms of Lys298 are positioned nearly in the middle of the electron density in the LTI model (Figure 3d), whereas those in the LTQ model are located in the periphery of the electron density (Figure 3b). The plane of the quinone ring is also better accommodated inside the electron density in the LTI model than in the LTQ model, and the planarity is extended to the CE atom of Lys298 (Figure 3d), which is permitted only for the sp^2 N^ϵ atom of LTI. These data strongly suggest that the cross-link formed between dopaquinone and Lys298 has an imine double bond character and the quinone is stabilized as LTI rather than LTQ.

Comparison of UV/Vis Spectra of D298K with Those of LTQ and LTI Model Compounds. Figure 4 shows the UV/vis spectra of an LTQ model compound, 5-*tert*-butyl-4-*N*-*n*-butylamino-1,2-benzoquinone at pH 7 and pH 11 (see Scheme 4). At physiological pH, the model compound is stabilized as an *o*-quinone with λ_{max} at 504 nm as seen in LTQ in LOX.³³ The pK_a of the amino group of the *n*-butylamino side chain of the related model compound, 5-ethyl-4-*N*-*n*-butylamino-1,2-benzoquinone has been determined to be 10.3 by UV/vis spectroscopic pH titration.²⁴ 5-*tert*-Butyl-4-*N*-*n*-butylamino-1,2-benzoquinone³⁴ was used in this study as the 5-ethyl-quinone was not stable in alkaline conditions. Upon deprotonation, a 50 nm blue-shift in λ_{max} was observed due to the formation of the monoanionic form of LTI (Scheme 4). The monoanionic form of LTI resembles the chromophore in D298K (Figure 2)

(33) Wang, S. X.; Nakamura, N.; Mure, M.; Klinman, J. P.; Sanders-Loehr, J. *J. Biol. Chem.* **1997**, 272 (46), 28841–28844.

(34) Culpepper, M. B.; Mure, M. Manuscript in preparation.

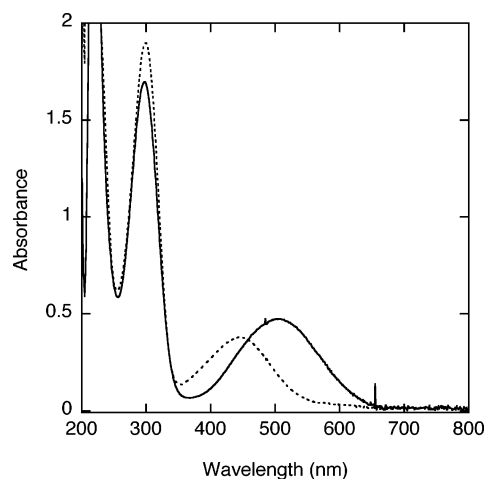
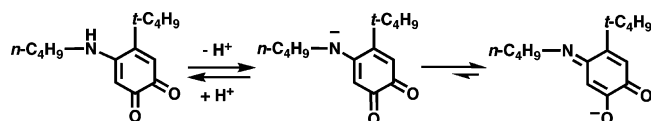


Figure 4. UV-vis spectra of LTQ and LTI (monoanionic form) model compounds. [LTQ] = 1.7 mM in 50 mM HEPES buffer, pH 6.8; [LTI] = 1.7 mM in 0.1 M NaOH. — LTQ, -----LTI.

Scheme 4. Acid Dissociation of LTQ to Form the Monoanionic Form of LTI in the Model System



although it lacks the large absorption around 320 nm. Nonetheless, the visible spectrum of D298K is similar to that of the monoanionic LTI, supporting the assignment of the quinone in D298K as the iminoquinone tautomer of LTQ. The differences in the UV spectrum between D298K and the model compound may arise from the difference in protonation states, where the quinone in D298K would be expected to be neutral as opposed to monoanionic.

Effect of pH on the UV/Vis Spectrum of D298K. It has been shown in model studies that the C5 carbonyl group of TPQ undergoes nucleophilic addition of substrates and inhibitors, whereas the C2 carbonyl group is unreactive.³⁵ The C2 carbonyl group is less electrophilic than that at C5 due to the resonance delocalization of the O4 oxoanion at physiological pH. This selective reactivity of nucleophiles at C5 of the TPQ cofactor over that at C2 has been also confirmed in CAO.¹ In addition to the resonance effect, the C5 carbonyl group is located near the proposed substrate entry channel⁸ and the active-site base, Asp298, for optimal activity. For this reason, it is less likely that the C2 carbonyl group of the TPQ cofactor reacts with the ϵ -amino side chain of Lys298 to form LTI in D298K. Alternatively, it could be possible that TPQ is formed initially in D298K but the C5 carbonyl group of TPQ reacted with ϵ -amino side chain of Lys298 to form an iminoquinone similar to the substrate Schiff base intermediate in the catalytic cycle.^{1,35} If so, the C5 imino group should be sensitive toward alkaline hydrolysis. To test for this possibility, D298K was incubated in pH 10 buffer and 1 M KOH. Under these conditions, we did not see any red-shift of λ_{\max} to 480 nm, suggesting that the hydrolysis to TPQ did not occur (data not shown). This is consistent with the cross-link between the ϵ -amino side chain of Lys298 and the quinone being at the C2 position, as revealed by the X-ray crystal structure.

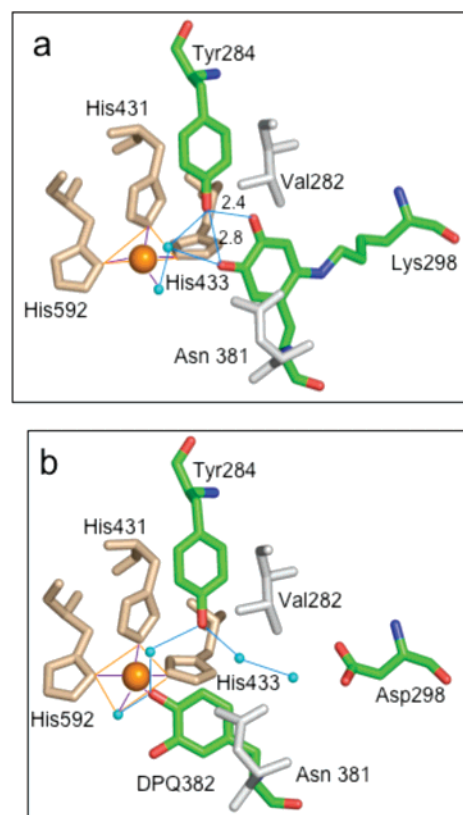


Figure 5. Active-site structure of D298K and the putative dopaquinone intermediate seen in TPQ biogenesis in WT. (a) D298K, (b) dopaquinone intermediate.⁹ Copper is shown as a golden sphere, and water molecules are shown in light-blue spheres. Val282 and Asn381 forming a wedge-shape pocket are shown in gray.²¹ Figures are generated by Pymol (DeLano Scientific LLC, <http://www.pymol.org>).

Effect of Disrupting the Hydrogen-Bonding Interaction between O4 and Tyr284 on the UV/Vis Spectrum of D298K.

The X-ray crystal structure of D298K (Figure 5) suggested a strong hydrogen-bonding interaction between O4 of the quinone and the conserved Tyr284 (Scheme 3). In order to assess whether this hydrogen-bonding interaction contributes to stabilizing the LTI tautomer in D298K, we disrupted the interaction by denaturation with 8 M urea at pH 7. The denaturation yielded a drastic spectral change to form a large absorbance around 350 nm but almost no absorbance above 450 nm (data not shown). Interestingly, a very similar spectral change was observed upon copper removal from LOX isolated from bovine aorta in 6 M urea where the 350 nm species was proposed to be derived from the modification of the LTQ with an amino acid side chain.²⁹ It could be possible that a similar modification took place on the LTQ-like quinone in denatured D298K.

In order to define the role of the hydrogen bond between Tyr284 and the O4 of the quinone in D298K in stabilizing LTI over LTQ, we prepared a double mutant Y284F/D298K. This double mutant was positive for quinone staining (SI Figure 4) but did not react with phenylethylamine and hydrazines as in the case of D298K. The UV/vis spectrum of Y284F/D298K has a broad absorbance at 504 nm very similar to that of the LTQ cofactor (Figure 6).²⁴ This red-shift compared to that from the quinone in D298K would be expected if the LTQ tautomer dominated the equilibrium. Further characterization of this mutant was not possible due to the instability of the quinone to

(35) Mure, M.; Klinman, J. P. *J. Am. Chem. Soc.* **1995**, *117* (34), 8707–8718.

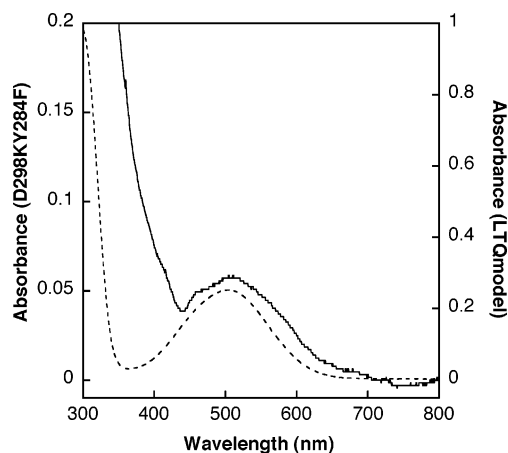


Figure 6. UV/vis spectra of Y284F/D298K and an LTQ model compound. [LTQ] = 1.7 mM, [Y284FD298K] = 0.1 mM in 50 mM HEPES buffer, pH 6.8. — Y284F/D298K, -----LTQ model.

form a 350-nm species similar to that seen in urea denaturation of D298K discussed above.

Biogenesis of LTI in D298K. The time course of LTI formation in D298K at pH 6.8 was followed by UV/vis spectroscopy (Figure 7). The apo-D298K was prepared by the standard procedure used to prepare apo-WT.^{3,22} The apo-D298K was mixed with a Cu^{2+} solution at saturating concentrations of O_2 (1.1 mM at 30 °C). Initially (<15 min), a pink species (broad absorption at ~500 nm) was formed, and then the absorption at >500 nm slowly decreased (~4 h to completion) concomitant with the increase in absorbances at 454 and 320 nm to give a final spectrum that is identical to that of LTI in the holo-D298K described above. An isosbestic point at 487 nm was observed for the conversion of the ~500 nm species to the 454-nm species. The rate of formation of the 500 nm species is 0.24 min^{-1} at pH 6.8, and this rate is about 1/6 of the rate of TPQ biogenesis in WT (1.50 min^{-1}).¹¹ The 500 nm intermediate could be either TPQ which then reacts with the lysine side chain to form the cross-link, or it could be an LTQ-like quinone that slowly converts to the LTI tautomer (Scheme 5). In both of these cases, there is an O_2 -dependent step (formation of the 500 nm species) and O_2 -independent step (formation of LTI from the 500 nm species). When the biogenesis reaction was performed at atmospheric O_2 concentrations ($225 \mu\text{M}$ at 30 °C), the rate of formation of the 500 nm species decreased to 0.05 min^{-1} , but the rate of the formation of LTI was unchanged versus saturated O_2 (Table 2). This is consistent with both of the possible mechanisms for the formation of LTI from the 500 nm species.

In order to gain insight into the identity of the 500 nm species observed at the early stage of the biogenesis, we first incubated the sample at 10 min with 2-hydrazinopyridine. No reaction was observed, indicating that the species is not TPQ (data not shown). We then followed the course of the biogenesis of the quinone in D298K by resonance Raman spectroscopy ($[\text{O}_2] = 225 \mu\text{M}$) (SI Figure 5). Under the reaction conditions used for resonance Raman spectroscopy, the rate of the biogenesis was significantly slower [most likely due to high concentration of enzyme (1 mM) used where O_2 becomes a limiting reagent], but the overall trends of the spectral change were similar to what was observed in the UV/vis spectroscopy experiment. During the initial phase of the biogenesis, peaks at 1186, 1364,

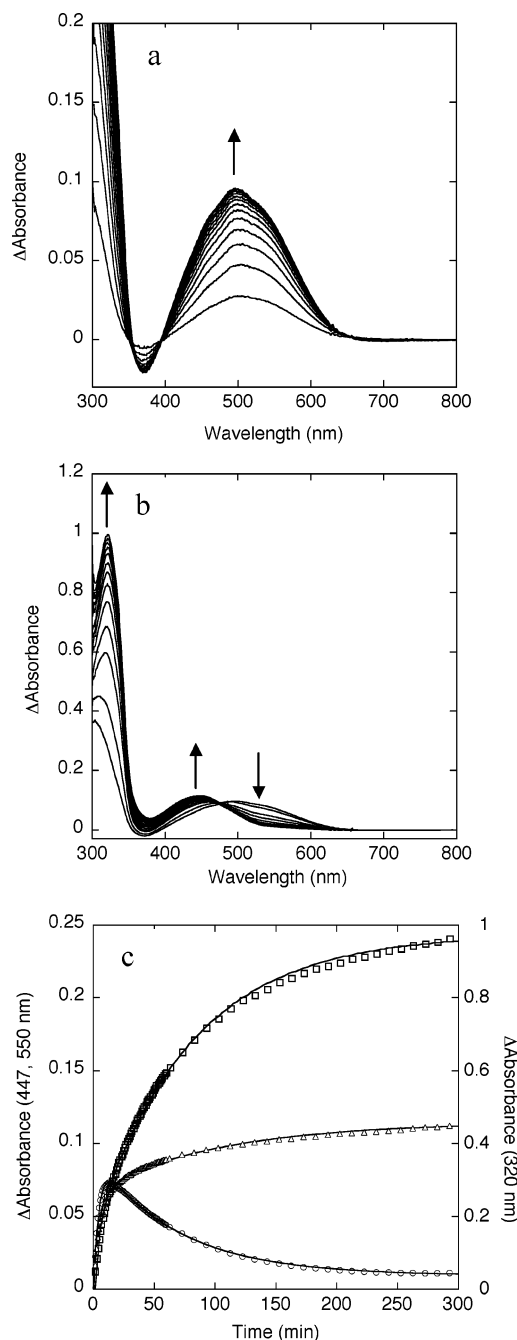
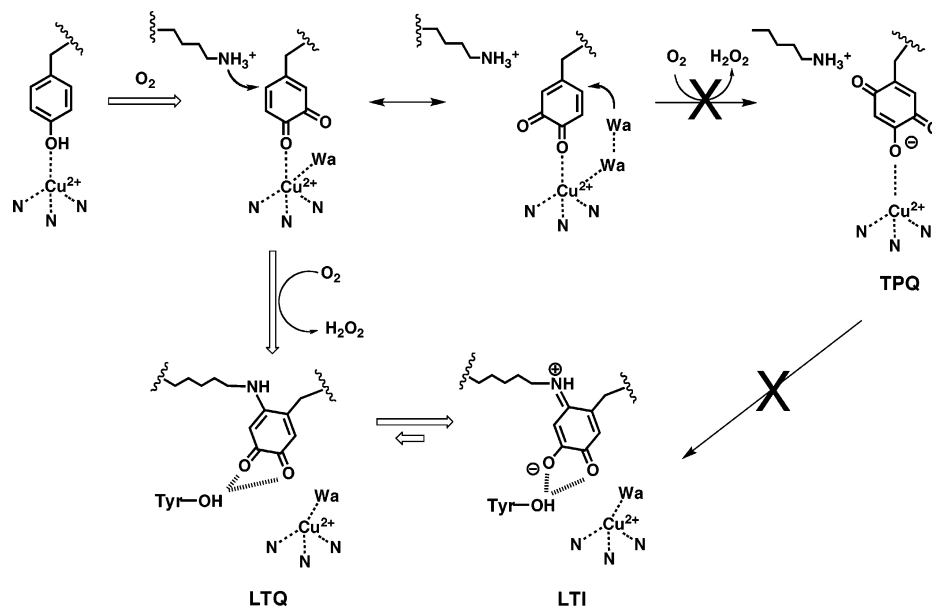


Figure 7. UV/vis spectral changes after addition of Cu^{2+} to apo-D298K under O_2 -saturating conditions ($[\text{O}_2] = 1.1 \text{ mM}$) at 30 °C. a) First phase: absorption spectra were recorded at 0, 2, 4, 6, 10, 20, 40 min, 1 h. b) Second phase: absorption spectra were recorded at 1, 2, 3, 6 h. Arrows indicate the direction of the spectral changes. c) Absorbance changes at 320 (□), 454 (Δ), 550 nm (○) were plotted against time and fitted to sum of two exponentials by the least-square method (see Table 2).

1393, 1554, 1688 cm^{-1} appeared where these species were associated with the 500 nm species (SI Figure 5). As the absorbance at ~500 nm decays, the peaks at 1186, 1554, and 1688 cm^{-1} then disappeared, and therefore, they are likely derived solely from the 500 nm intermediate. The peaks observed during the biogenesis at 1364 and 1393 cm^{-1} are very close in energy to those associated with holo-D298K (at 1361 and 1391 cm^{-1} , SI Figure 5), but the observed ratio of the two peaks is different: holo, $1361 < 1391$; intermediate, $1364 > 1393$. The resonance Raman spectra were all collected at an

Scheme 5. Possible Mechanisms for LTI Formation in D298K**Table 2.** Rates of Biogenesis of D298K

[O ₂]	first phase (min ⁻¹)	second phase (min ⁻¹)
1.1 mM	0.236 ± 0.004	0.015 ± 0.001
225 μM	0.050 ± 0.006	0.015 ± 0.003

excitation wavelength of 514.5 nm. We have attempted to excite at 457.9 nm but have so far been unable to obtain a spectrum. One interpretation of the resonance Raman spectrum at 6 h (holo-D298K) is that at 514.5 nm we are selectively probing the 500 nm species over LTI and are therefore observing a small amount of the 500 nm species that remains in equilibrium with LTI. This would explain the decrease in intensity of the features over time.

Figure 8 shows the comparison of D298K-500 nm species (c), holo-D298K (b), and WT-AGAO (TPQ) (a) in comparison to model compounds of LTQ (d) and monoanionic LTI (e). The D298K-500 nm species is clearly neither TPQ nor LTI, thereby making a biogenesis mechanism where TPQ is an intermediate less likely. The 500 nm species is very similar to the LTQ model compound but does have some minor differences. Most likely the protein environment is modulating the electronic structure of the quinone in the D298K-500 nm species, thereby making it difficult to compare directly to LTQ in solution.

Discussion

An intermediate assigned as dopaquinone has been observed in the biogenesis of TPQ using time-resolved X-ray crystallography. By analogy, dopaquinone has been suggested as an intermediate in LTQ biogenesis. Previous work using resonance Raman spectroscopy confirmed that the C2 oxygen of TPQ was derived from a solvent water molecule strongly supporting the proposed reaction mechanism involving 1,4-addition of water to the C2 position of a dopaquinone intermediate after flipping.⁷ In a model study of LTQ biogenesis, it was shown that 1,4-addition of an amine to the C2 position of dopaquinone forms the LTQ cofactor and the enzyme active site must be pre-organized to prevent a 1,2-addition reaction.²⁴ In order to understand the mechanism of TPQ and LTQ cofactor biogenesis, we have incorporated a lysine residue in the active site of AGAO

in two positions in an attempt to trap the dopaquinone intermediate either before flipping or after flipping and to generate a LTQ-like cofactor in CAO. On the basis of the model chemistry,²⁴ a correctly placed amine should be able to effectively trap the putative dopaquinone intermediate thereby forming an LTQ-like quinone.

The UV/vis and resonance Raman spectra of holo-D298K-AGAO indicated that it contained a quinone different from TPQ and LTQ, and the presence of a quinone in D298K was confirmed by the standard quinone-staining. The quinone was unreactive toward hydrazines, precluding further characterization by chemical means or by mass spectrometry as was previously used to identify TPQ in CAO and LTQ in LOX.^{2,23} However, we were able to obtain an X-ray crystal structure of D298K. The structure indicated the presence of a new quinone cofactor in AGAO where a cross-link had been formed between the C2 position of the quinone ring and the ε-amino side chain of Lys298 through 1,4-addition, but the resulting quinone was stabilized as an iminoquinone tautomer of LTQ (LTI) rather than an *o*-quinone (LTQ). The orientation of LTI in D298K is in a flipped, inactive conformation where the active carbonyl group at C5 is facing away from the proposed substrate entry channel.⁸ Because of this, D298K is not active toward oxidative deamination of substrate amine and does not react with inhibitors such as 4-nitrophenylhydrazine and 2-hydrazinopyridine. Most importantly, the combination of UV/vis and resonance Raman spectroscopies and the structural data strongly support the identity of the quinone in D298K as LTI.

In order to assess why LTI is stabilized over LTQ in the active site of D298K, we turned our focus to the hydrogen-bonding interaction (2.4 Å) between the O4 of LTI and Tyr284 (Figure 5) which is conserved among CAOs and is thought to play a key structural role in catalysis.^{21,36} We first incubated D298K in alkaline pH, but we did not observe any spectral change. Upon incubation in 8 M urea, the 450 nm absorbance disappeared, and a new peak at 350 nm appeared. It should be noted

(36) Mure, M.; Kurtis, C. R.; Brown, D. E.; Rogers, M. S.; Tambyrajah, W. S.; Saysell, C. G.; Wilmot, C. M.; Phillips, S. E. V.; Knowles, P. F.; Dooley, D. M.; McPherson, M. J. *Biochemistry* **2005**, *44*, 1583–1594.

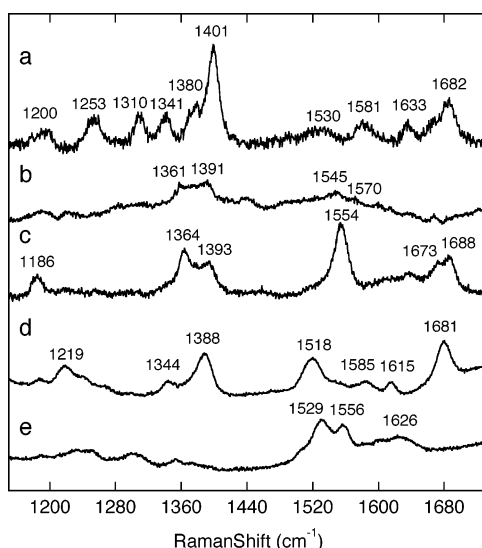


Figure 8. Resonance Raman spectra of holo-D298K, the 500-nm intermediate seen in the biogenesis of D298K, TPQ in WT, LTQ model compound in 50 mM HEPES, pH 6.8, and monoanionic form of LTI model compound in 0.1 M KOH. a) WT (TPQ), b) holo-D298K, c) the 500-nm intermediate, d) LTQ model compound, e) monoanionic form of LTI model compound. Excitation wavelength = 514.5 nm.

that a similar 350 nm species was observed upon incubation of LOX in 6 M urea and a copper chelator.²⁹ The nature of the 350 nm species is currently undefined, but it is most likely due to the covalent modification of the LTQ cofactor with a nucleophilic amino acid side chain that becomes available after urea denaturation. This result was promising but not definitive, so we prepared the double mutant Y284F/D298K. This mutant was not very stable so care had to be taken to minimize the time for protein purification. We were only able to prepare the holo form of double mutant by growing host cells (*E. coli*) in the presence of Cu^{2+} , and attempts to isolate and reconstitute apo-Y284F/D298K were unsuccessful. The UV/vis spectrum of the holo-Y284F/D298K was taken immediately after purification, and it had a visible spectrum very similar to that of LTQ (λ_{max} at 504 nm). The presence of a quinone was confirmed by the standard quinone staining, but Y284F/D298K was not reactive toward substrate amine and hydrazine inhibitors as in the case of D298K. This is predicted as the quinone has been fixed in the inactive orientation due to the cross-link, and therefore, the active carbonyl group at C5 is not accessible by nucleophiles. These results suggest that the quinone in D298K is stabilized as LTI through a hydrogen-bonding interaction with Tyr284 and such an interaction must be absent for the LTQ cofactor in LOX.

We next studied the biogenesis of LTI in D298K. In WT-AGAO, the formation of TPQ occurs directly from the Cu^{2+} -bound tyrosine precursor where no spectroscopic intermediates have been observed. The formation of TPQ is rapid and complete within a couple of minutes under saturating concentration of O_2 at pH 6.8. When apo-D298K was exposed to Cu^{2+} and then O_2 , the initial reaction did not produce LTI, but instead produced a pink species with a broad visible absorbance centered at ~ 500 nm. The formation of the 500 nm species was essentially complete within 15 min after which it slowly decayed over several hours. The decay was concurrent with the formation of LTI. The rate of formation of the 500 nm species is about 1/6 of that of TPQ in WT and no other spectroscopic intermedi-

ates were observed. This suggests that the rate-limiting step in the biogenesis of the 500 nm species in D298K versus TPQ in WT is the same. This is consistent with TPQ biogenesis in D298A where the removal of the carboxyl side chain of Asp298 has only a minimal effect on the rate of biogenesis of TPQ (40% reduction).²⁷

The 500 nm intermediate is not reactive toward hydrazines, suggesting that it is not TPQ. The resonance Raman spectrum of the 500 nm intermediate was compared with those of TPQ, LTI in D298K, and model compounds of LTQ and the monoanionic form of LTI. The 500 nm species is distinct from TPQ, thereby ruling out a mechanism where the ϵ -amino side chain reacts with C2 carbonyl of TPQ to form the iminoquinone. This was expected as the C2 carbonyl of TPQ is intrinsically unreactive.^{1,35} The cross-link has most likely already formed in the 500 nm species from the reaction of the amine with dopaquinone. The resonance Raman of the 500 nm species has features of LTQ but not LTI, and so we have tentatively assigned this as an LTQ-like quinone. The spectral differences between LTQ and the LTQ-like quinone in D298K may be caused by differences in their electronic structures dictated by interactions between the quinone and the active site in D298K. On the basis of our observation that the LTI tautomer is stabilized by a hydrogen-bonding interaction with Tyr284, we propose that the slow conversion of the 500 nm species to LTI is controlled by a subtle conformational change in the active site where LTI is the thermodynamic product in D298K.

The mobility of TPQ and TPQ-derived reaction intermediates in CAOs are tightly controlled by hydrogen-bonding interactions, particularly between the O4 of TPQ and the conserved Tyr (Tyr284 in AGAO) for optimal activity.²¹ The TPQ ring is located in a wedge-shaped cavity in the active site, but the mobility is limited to pivoting inside of the wedge.^{21,28} When these hydrogen-bonding interactions are disrupted by high salt, decreasing pH, or site-directed mutagenesis, the TPQ ring gains mobility and swings out from the wedge and can ultimately be trapped by ligation to the active-site Cu^{2+} , all of which lead to greatly reduced catalytic activity. In contrast to mature TPQ, the possible mobility of the reaction intermediates in the TPQ biogenesis has not been considered. From the X-ray snapshot analysis, the precursor Tyr382 is initially bound to the Cu^{2+} residing outside the active-site wedge (Figure 1a).⁹ The proposed dopaquinone intermediate and trihydroxybenzene form of TPQ (TPQ_{red}) are both still interacting with Cu^{2+} (Figure 1b,d). Upon oxidation of TPQ_{red} to TPQ_{ox}, TPQ finally leaves the active-site Cu^{2+} and swings into the wedge to be captured by Tyr284 to be in the active conformation (Figure 1e). It is not known what factors cause TPQ_{ox} to leave the Cu^{2+} site. The present study of D298K clearly showed that the proposed dopaquinone intermediate (Figure 1b) has mobility and can leave the Cu^{2+} site and swing into the active-site wedge to react with Lys298. An attempt was made to trap the dopaquinone with a lysine residue incorporated at position 602 in AGAO (M602K). Met602 is on the opposite side of the active site compared to Asp298 and, should a cross-linked quinone be formed, would be expected to be in an active conformation. However, the holo-M602K contained TPQ where no such cross-link formed. The most likely explanation for this is that the lysine (Lys602) is not accessible to the C2 position of the flipped dopaquinone and thereby cannot compete effectively with hydration.

An important observation from this study is the absence of any detectable amount of TPQ in D298K. The active site of AGAO is arranged to optimize the 1,4-addition of copper-associated water to dopaquinone intermediate to form TPQ. A recent model study suggested that an appropriately placed Cu^{2+} ion can catalyze the 1,4-addition of water to dopaquinone.³⁷ The mutation site to incorporate the lysine residue in D298K is away from the copper site, and it is less likely that the environment around copper is significantly altered when compared to that of WT. The rate of formation of the 500 nm species is close to that of WT and D298A suggesting that initial steps of biogenesis, activation of Tyr382 and subsequent oxidation to dopaquinone, are not perturbed in D298K. However, in D298K the dopaquinone intermediate is selectively trapped by the amino group of Lys298 to form LTI. This suggests that 1,4-addition of the ϵ -nitrogen of Lys298 to the dopaquinone intermediate in CAO is much more efficient than the addition of copper-associated water, even though the latter is the natural reaction. A similar phenomenon was observed in the model study of the LTQ biogenesis, where dopaquinone can be trapped efficiently by secondary alkyl amines to form LTQ, but not by solvent water to form TPQ.²⁴ In this model study, primary amines reacted rapidly with the carbonyl groups of dopaquinone in preference to 1,4-addition. That such chemistry did not occur in D298K and is also not seen in LOX strongly suggests that the positioning of the reactive amine in the active site is key in

controlling the chemistry (1,4- vs 1,2-addition and hydration vs amination).

Conclusion

In summary, we have reported the chemical trapping of the dopaquinone intermediate in the biogenesis of TPQ. These results support the intermediacy of dopaquinone in TPQ biogenesis and also provide the first enzymatic evidence that dopaquinone is also an intermediate in LTQ biogenesis. Appropriately placed, an ϵ -amino side chain of lysine residue can effectively compete with a water molecule to prevent hydration and inhibit formation of TPQ, even when the active site is optimized for the latter reaction. Finally, there is an intrinsic mobility for the biogenic intermediates in TPQ biogenesis that parallels the mobility of TPQ and the reaction intermediates in the catalytic cycle. The control of this mobility by the protein is an essential feature of the biogenesis reaction.

Acknowledgment. This study was supported by NIH COBRE Award 1 P20RR15563 and matching support from the State of Kansas (to M.M.) and Grants-in-Aid for Scientific Research from the Ministry of Education, Culture, Sports, Science and Technology of Japan (Category B, 18370043 and 18350085 to K.T. and T.O., respectively). M.M. thanks Julian Limburg for critical reading of the manuscript and valuable discussions.

Supporting Information Available: Five additional figures. This material is available free of charge via the Internet at <http://pubs.acs.org>.

JA0731165

(37) Ling, K.-Q.; Sayre, L. M. *J. Am. Chem. Soc.* **2006**, *127*, 4777–4784.